

Biophysical Journal, Volume 113

Supplemental Information

**Biphasic Effect of Profilin Impacts the Formin mDia1 Force-Sensing
Mechanism in Actin Polymerization**

**Hiroaki Kubota, Makito Miyazaki, Taisaku Ogawa, Togo Shimosawa, Kazuhiko Kinoshita,
Jr., and Shin'ichi Ishiwata**

SUPPLEMENTAL MATERIALS AND METHODS

Plasmid construction

The nucleotide sequences corresponding to the 650-amino acid (aa) sequence of mammalian homolog of diaphanous 1 (mDia1), including FH1 and FH2 (residues 543–1192), from mouse cDNA were cloned into the pGex6P-1 vector (GE Healthcare, Buckinghamshire, UK) between *Bam*HI and *Xho*I sites and expressed as an N-terminally GST-tagged fusion protein. The truncated mDia1 (650 aa) was used in previous studies (1,2) and was designated mDia1 Δ N3. In the present study, the expressed protein was simply referred to as mDia1.

Full-length profilin I from mouse cDNA was cloned into the pRSET-A vector (Life Technologies, CA, USA) between its *Nde*I and *Eco*RI sites and was expressed without the His-tag.

Protein preparation

Truncated mDia1 expressed in *Escherichia coli* Rosetta II competent cells (Merck Millipore, Bellerica, MA, USA) was purified using Glutathione-Sepharose HP resin (GE Healthcare), as previously reported (1). Profilin I was expressed in *E. coli* Rosetta II cells and purified using poly-L-proline sepharose according to previous reports (3,4). Poly-L-proline sepharose was prepared by coupling poly-L-proline (Sigma-Aldrich, St. Louis, MO, USA) with cyanogen bromide (CNBr)-activated sepharose (GE Healthcare). The concentrations of mDia1 and profilin were measured by the Bradford assay based on a standard curve obtained with bovine serum albumin (BSA; Sigma-Aldrich). Purified proteins were stored at -80°C .

G-actin was purified from acetone powder prepared from rabbit skeletal muscle, as previously reported (5), and was stored in ATP-G-buffer (2 mM Tris-HCl [pH 8.0], 2 mM NaN_3 , 50 μM CaCl_2 , and 0.1 mM ATP) at -80°C . For actin preparation, all procedures conformed to the Guidelines for Proper Conduct of Animal Experiments approved by the Science Council of Japan and were performed according to the Regulations for Animal Experimentation at Waseda University. For microscopic analysis, the G-actin solution was thawed and polymerized by adding one-fifth volume of 5 \times ATP-F-buffer (500 mM KCl, 10 mM MgCl_2 , 10 mM 3-morpholinopropanesulfonic acid [MOPS, pH 7.0], and 7.5 mM NaN_3). After centrifugation ($436,000 \times g$, 30 min, 8°C), the precipitated F-actin was dialyzed against ATP-G-buffer and centrifuged again ($436,000 \times g$, 30 min, 2°C). The supernatant was used in the experiment with ATP-G-actin within 1 week. The concentration of G-actin was calculated by dividing its absorbance at 290 nm by $0.63 (\text{mg}/\text{mL})^{-1}$. For preparation of ADP-G-actin, an equal volume of 2 \times ADP-F-buffer (20 mM imidazole-HCl [pH 7.0], 200 mM KCl, 2 mM MgCl_2 , 0.4 mM EGTA, 0.2 mM ADP, 2 mM dithiothreitol [DTT], 10 mM glucose, and 15 U/mL hexokinase [Sigma-Aldrich]) was added to the preserved ATP-G-actin (1 mg/mL), with incubation for 30 min at room temperature ($24 \pm 2^{\circ}\text{C}$) for polymerization. After centrifugation ($436,000 \times g$, 30 min, 4°C), the pellet was resuspended in ADP-G-buffer (2 mM Tris-HCl [pH 8.0], 0.1 mM CaCl_2 , 0.2 mM ADP, 1 mM DTT, 5 mM glucose, 15 U/mL hexokinase, and 25 μM Ap5A [Sigma-Aldrich]), briefly sonicated (5 s), and incubated on ice for 1 h. The prepared ADP-G-actin was used within 3 h.

Fluorescently labeled actin filaments (10% biotinylated) were prepared as described previously (6).

Preparation of IC5-labeled avidin beads

Since two types of 1- μ m beads (mDial-immobilized and neutravidin-coated beads, referred to as “mDial beads” and “avidin beads”) were present in the assay solution, these two types of beads had to be distinguished somehow during microscopic analysis. Therefore, the avidin beads were labeled with another fluorescent dye, IC5, which has fluorescent properties ($\lambda_{\text{ex}} = 640$ nm, $\lambda_{\text{em}} = 660$ nm) different from those of rhodamine ($\lambda_{\text{ex}} = 540$ nm, $\lambda_{\text{em}} = 565$ nm). IC5-conjugated BSA and neutravidin were bound to 1- μ m beads at the same time for fluorescent labeling with IC5. Thus, red laser light (633 nm) excited the avidin beads, but not the mDial beads, allowing for discrimination between the two types of beads. Furthermore, the avidin beads could also be excited by green laser light (532 nm), which excited rhodamine-labeled short actin filaments due to the fluorescence of 1- μ m beads. This situation was convenient for manipulations involving connection of short actin filaments to the avidin beads. IC5 labeling of BSA was performed using IC5-maleimide (Dojindo, Kumamoto, Japan).

Immobilization of IC5-conjugated BSA and neutravidin on carboxylate-modified 1- μ m polystyrene beads (F8814 blue fluorescent microspheres; Life Technologies) was performed by amine coupling, as previously reported (7,8). First, a precipitate from 50 μ L of beads obtained by centrifugation ($16,000 \times g$, 1 min, 4°C) was resuspended and washed with 1 mL of 0.1 M sodium carbonate buffer (pH 9.6) three times. Next, the beads were washed with 1 mL of 20 mM sodium phosphate buffer (pH 4.7) three times and resuspended in 100 μ L of 20 mM sodium phosphate buffer (pH 4.7). Next, 20 μ L of 2 M ethylene dichloride (EDC; Thermo Fisher Scientific, Waltham, MA, USA) in 0.5 mM MOPS buffer (pH 7.0) was added to the resuspended beads, and the mixture was incubated at room temperature for 20 min, followed by addition of 40 μ L of 2 M N-hydroxysulfosuccinimide (Sulfo-NHS; Thermo Fisher Scientific) and incubation at room temperature for 20 min. Then, after washes with 1 mL of 200 mM sodium borate buffer (pH 8.4) three times, the beads were resuspended in 100 μ L of 200 mM sodium borate buffer (pH 8.4) and incubated overnight at 4°C after the addition of 20 μ L of 5 mg/mL neutravidin (Life Technologies) and 2 μ L IC5-conjugated BSA (~10 mg/mL). After quenching of the reaction by addition of 250 mM 2-ethanolamine and incubation at 4°C for 30 min, the beads were washed with 1 mL of 2 mg/mL BSA in 200 mM sodium borate buffer (pH 8.4) three times. Finally, the beads were resuspended in 200 μ L of 20 mM sodium phosphate buffer (pH 7.4) containing 1 mg/mL BSA, 15 mM NaCl₂, 15 mM NaN₃, and 5% (v/v) glycerol. The prepared avidin beads were kept on ice and used within 3 weeks.

Conjugation of glutathione to BSA

For conjugation of glutathione to BSA without reducing the affinity for GST, the SH group of reduced glutathione (GSH) must be covalently linked to BSA via a maleimide group. After blocking of the SH groups of BSA (35 groups per molecule) by N-ethylmaleimide, an amino

group of blocked BSA was linked to a N- γ -maleimidobutyryl-oxysuccinimide ester (GMBS) crosslinker, allowing for protrusion of the reactive maleimide group from BSA, to which GSH could be attached. Briefly, 0.2 mL of 1.1 mM N-ethylmaleimide (NEM) in dimethylformamide was added to 2 mL of 50 mg/mL BSA (Sigma-Aldrich) in HEPES-EDTA buffer (100 mM HEPES-KOH [pH 7.2] and 10 mM EDTA), which was gently stirred, and the mixture was incubated at room temperature for 90 min. Next, the mixture was dialyzed against 1 L of HEPES-EDTA buffer overnight at 4°C. The volume of the sample solution increased approximately 1.2-fold during the dialysis, yielding a BSA solution with a concentration of approximately 40 mg/mL. After dialysis, 200 μ L of the sample was mixed with 800 μ L of HEPES-EDTA buffer, and the mixture was then incubated with stirring at room temperature for 30 min after addition of 100 μ L of 110 mM GMBS (Thermo Fisher Scientific). Next, 1.1 mL of 0.2 M GSH in HEPES-EDTA buffer was added to the sample, and the mixture was incubated at room temperature for 1 h, followed by dialysis against 20 mM Tris-HCl (pH 7.5) with 100 mM KCl. The concentration of glutathione-conjugated BSA estimated in its final volume was approximately 6 mg/mL. The prepared glutathione-conjugated BSA was rapidly frozen by liquid nitrogen and stored at -80°C .

Preparation of the mDia1 beads via the GST-glutathione interaction

After mixing 2 μ L of 1- μ m polystyrene beads (F8814 blue fluorescent microspheres; Life Technologies) with 18 μ L HEPES-EDTA buffer (100 mM HEPES-KOH [pH 7.2] and 10 mM EDTA), 15 μ L of the mixture was added to 15 μ L of glutathione-conjugated BSA (\sim 6 mg/mL), and the mixture was incubated at room temperature for 15 min. Next, 100 μ L of 10 mg/mL BSA in Basic buffer (50 mM KCl, 10 mM imidazole-HCl [pH 7.4], 1 mM MgCl_2 , 1 mM EGTA, and 50 μ M CaCl_2) was added, followed by incubation at room temperature for 5 min. After centrifugation ($16,000 \times g$, 1 min, 4°C), the precipitated beads were resuspended in 100 μ L of 10 mg/mL BSA in Basic buffer. The beads were washed three times using this process and resuspended in 300 μ L of 10 mg/mL BSA in Basic buffer. Next, 1.5 μ L of 270 nM mDia1 was added to the beads with incubation on ice overnight. After centrifugation ($16,000 \times g$, 1 min, 4°C) and four washes with 300 μ L of 10 mg/mL BSA in Basic buffer, the precipitated beads (mDia1 beads) were resuspended in 300 μ L of 10 mg/mL BSA in Basic buffer and subjected to microscopic analysis within 1 day.

Supporting References

1. Higashida, C., T. Miyoshi, A. Fujita, F. Ocegüera-Yanez, J. Monypenny, Y. Andou, S. Narumiya, and N. Watanabe. 2004. Actin polymerization-driven molecular movement of mDia1 in living cells. *Science*. 303:2007–2010.

2. Mizuno, H., C. Higashida, Y. Yuan, T. Ishizaki, S. Narumiya, and N. Watanabe. 2011. Rotational movement of the formin mDia1 along the double helical strand of an actin filament. *Science*. 331:80–83.
3. Tuderman, L., E.R. Kuutti, and K.I. Kivirikko. 1975. An affinity-column procedure using poly(L-proline) for the purification of prolyl hydroxylase. Purification of the enzyme from chick embryos. *Eur. J. Biochem.* 52:9–16.
4. Kaiser, D.A., P.J. Goldschmidt-Clermont, B.A. Levine, and T.D. Pollard. 1989. Characterization of renatured profilin purified by urea elution from poly-L-proline agarose columns. *Cell Motil. Cytoskeleton.* 14:251–262.
5. Kondo, H., and S. Ishiwata. 1976. Uni-directional growth of F-actin. *J. Biochem.* 79:159–171.
6. Uemura, S., H. Higuchi, A.O. Olivares, E.M. De La Cruz, and S. Ishiwata. 2004. Mechanochemical coupling of two substeps in a single myosin V motor. *Nat. Struct. Mol. Biol.* 11:877–883.
7. Shimozawa, T., and S. Ishiwata. 2009. Mechanical distortion of single actin filaments induced by external force: detection by fluorescence imaging. *Biophys. J.* 96:1036–1044.
8. Oguchi, Y., S. Uchimura, T. Ohki, S.V. Mikhailenko, and S. Ishiwata. 2011. The bidirectional depolymerizer MCAK generates force by disassembling both microtubule ends. *Nat. Cell Biol.* 13:846–852.
9. Dupuis, D.E., W.H. Guilford, J. Wu, and D.M. Warshaw. 1997. Actin filament mechanics in the laser trap. *J. Muscle Res. Cell Motil.* 18:17-30.
10. Jégou, A., M.F. Carlier, and G. Romet-Lemonne. 2013. Formin mDia1 senses and generates mechanical forces on actin filaments. *Nat. Commun.* 4:1883.
11. Paul, A.S., and T.D. Pollard. 2008. The role of the FH1 domain and profilin in formin-mediated actin-filament elongation and nucleation. *Curr. Biol.* 18:9-19.

Figure S1

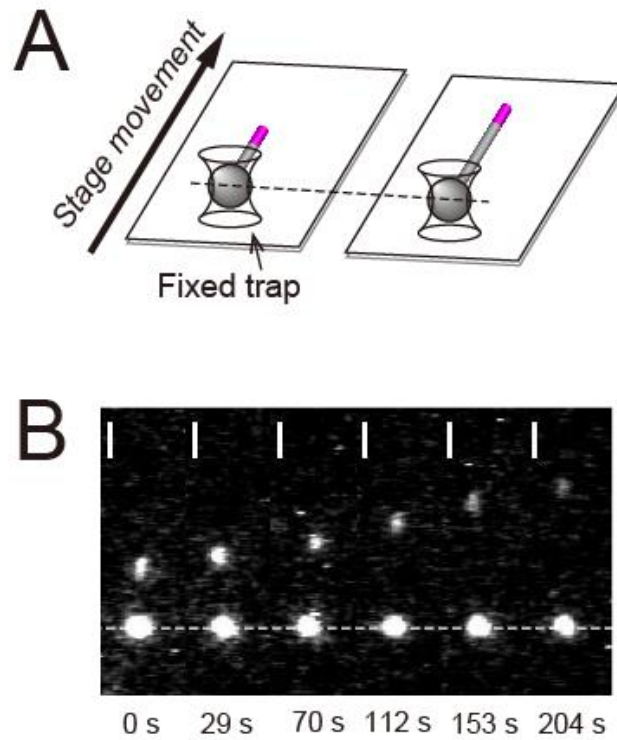


Figure S1. Fluorescent images showing the tip of the actin filament moving away from the mDia1 bead.

(A) Schematic illustration of the experiment showing actin polymerization from the mDia1 bead. While the mDia1 bead (gray sphere) was trapped by optical tweezers, the stage of the microscope was moved at a constant speed. The distance between the fluorescently labeled tip (magenta part) and the mDia1 bead increased with time because of the successive polymerization of unlabeled G-actin at the barbed end. (B) Fluorescent images showing elongation of the actin filament from the mDia1 bead (lower object). These images correspond to Supplementary **Movie 1**. The vertical scale bars are 2 μm .

Figure S2

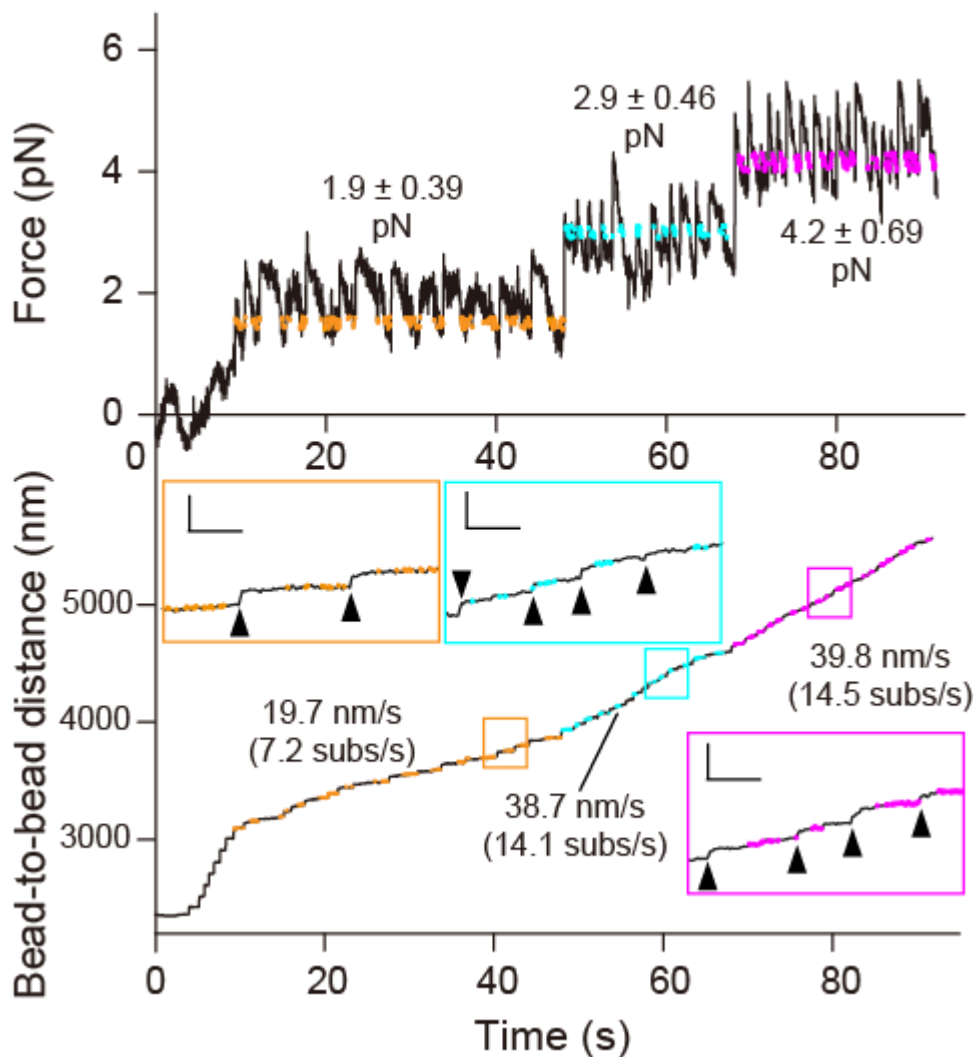


Figure S2. Estimation of the tensile force and elongation rate in the double-trap experiment. Two processes, i.e., extension of the distance between the trap centers via manipulation to maintain the tensile force nearly constant and relaxation of the tensile force due to elongation of the actin filament via polymerization, were repeated several times in the double-trap experiment. The trap centers were manually (not automatically) manipulated to keep the applied force nearly constant during elongation of the actin filament, and the tensile force could be approximately maintained. Almost all the experiments were conducted in the range of strong force (3.5–5.5 pN) to be compared with the data from single-trap experiments, whereas at a specific protein concentration, the double-trap experiments were performed in two other ranges of the tensile force: 2.0–3.5 pN as a moderate force and 1.0–2.0 pN as a weak force. To minimize the effects of rotation of beads on the measurement of bead-to-bead distance, plots with a limited tensile force were linearly fitted for estimation of the elongation rate. The plots in the ranges 1.4–1.6 (orange plots), 2.9–3.1 (cyan plots), and 4.0–4.2 pN (magenta plots) were used for linear fitting for the experiments under weak-, moderate-, and strong-force conditions, respectively. The partial time courses of these three force ranges are shown as enlarged views (insets surrounded by orange, cyan, magenta

rectangles), and arrowheads show the instantaneous changes of bead-to-bead distance due to the shift of trap center. Vertical and horizontal scale bars in insets are 100 nm and 1 sec, respectively. Although the elongation rate was estimated with the limited plots, the corresponding tensile force was obtained by averaging all continuous plots throughout the period in question (from the first to the last plots for estimation of the elongation rate). The present figure corresponds to 0.2 μM ATP-G-actin and 6 μM profilin.

Figure S3

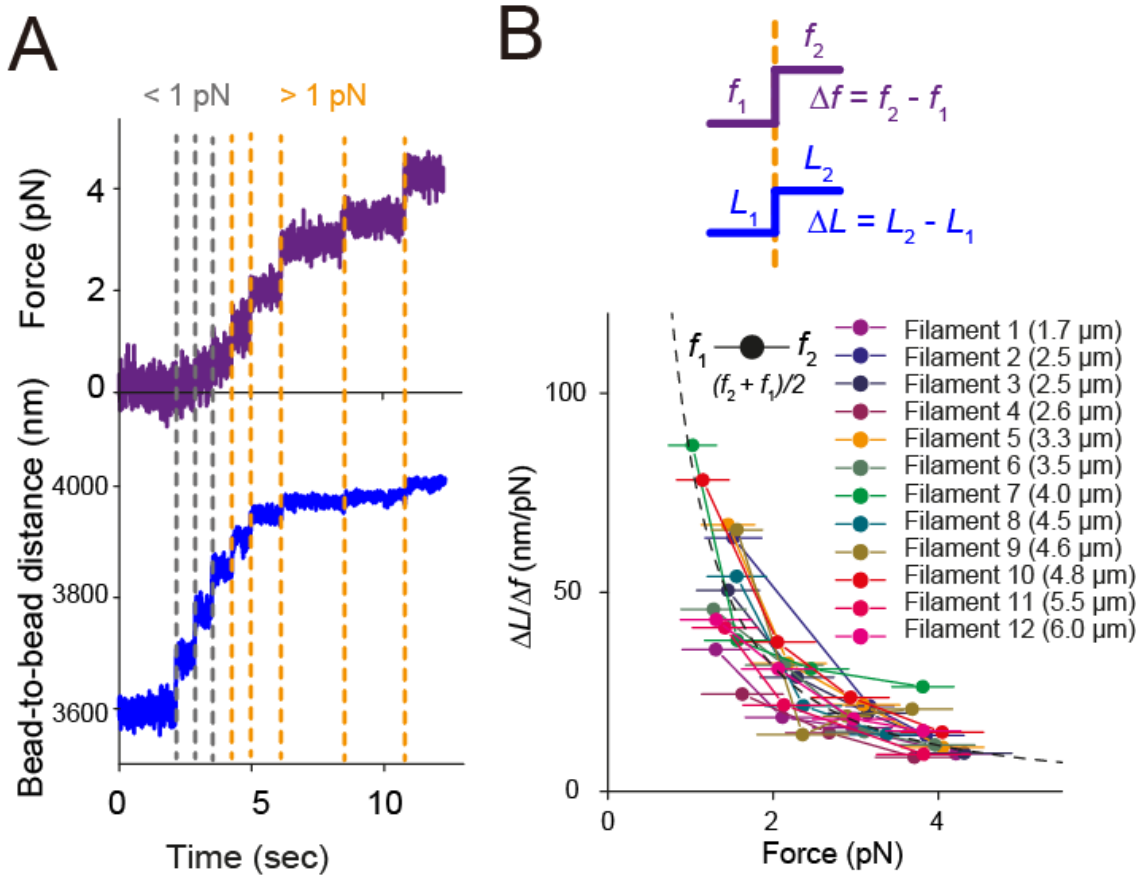


Figure S3 Force-dependent and actin polymerization-independent change of the bead-to-bead distance.

(A) A typical example of the change of the bead-to-bead distance caused by shifting the trap center. The double-trap experiment was performed at a low concentration of ATP-G-actin (75 nM) at which actin polymerization was slow (1.6 subunits/sec = 4.4 nm/sec at 4-pN pulling force, estimated from Fig. 3A) to measure the actin polymerization-independent change of the bead-to-bead distance. When one of the trap center trapping the mDia1 bead was shifted, the bead-to-bead distance instantaneously changed (gray and orange vertical broken lines). Stiffness of the laser trap was 0.024 pN/nm. (B) Non-linear relationship between stretching tension and the mechanical compliance (the reciprocal of stiffness) of actin dumbbells. The mechanical compliance ($\Delta L/\Delta f$) calculated from f_1 , f_2 (the average forces for 0.1-sec period before and after the shift of the trap center, respectively), and L_1 , L_2 (the bead-to-bead distances before and after the shift of the trap center, respectively) was plotted against the averaged force $(f_2 + f_1)/2$. Left and right sides of horizontal error bars are f_1 and f_2 , respectively. Twelve

independent experiments were performed with different lengths of actin filaments. The bead-to-bead distance just after the application of stretching tension that reached >2.0 pN (2.1-2.9 pN) is shown in parentheses. Only the events at which the averaged force $(f_2 + f_1)/2$ was greater than 1 pN (orange broken lines in **Fig. S3A**) were analyzed, because 1 pN is the minimum value for the measurement of actin filament elongation rate in the double-trap experiment. Results of all twelve filaments were fitted with a single equation that describes non-linear property of dL/dF arising from force-dependent rotation of beads in actin dumbbells (9), with an optimal flexural rigidity (EI) value (33,900 pN nm²). The fitting curve is shown as a broken line.

Figure S4

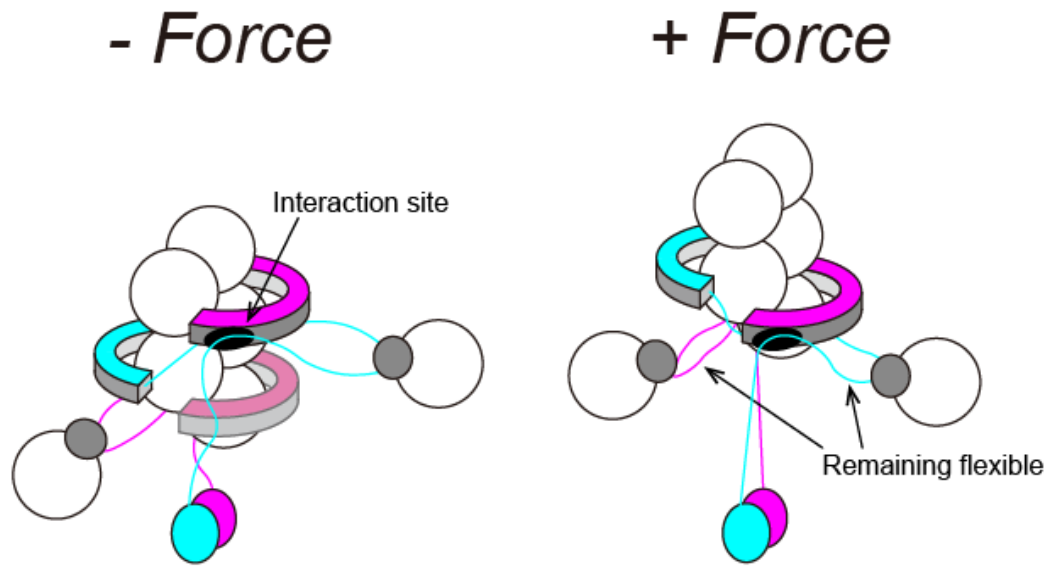


Figure S4 Possible structural change of FH1 domain by stretching tension. As proposed by Jégou et al. (10), one of the polyproline helices in the FH1 domain possibly interacts with alpha helices in the FH2 domain (shown as “Interaction site”). Six or 14 polyproline tracks are located at the FH1 domain of mDia1 (11). If the interaction remains under tension, stretching tension is transmitted directly from the GST dimer to the FH2 domain without affecting the flexibility of the FH1 structure, including other polyproline helices that bind profilin-actin complexes. This geometry allows the capture and delivery system to work under tension.

Captions for Movies

Movie 1. Fluorescent images of elongation of the actin filament from the mDial bead. The stage of the microscope was horizontally moved upward in the image while the mDial bead (the lower one) remained trapped. The object moving upward was the fragment of a fluorescently labeled short actin filament. The unlabeled actin filament bridged it with the mDial bead and elongates with time. The scale bar is 2 μm .

Movie 2. Phase contrast images of elongation of the bead-to-bead distance due to actin polymerization (0.2 μM ATP-G-actin). In each movie, phase contrast images of beads are shown on the left side, while the center of the lower bead calculated by means of the PTA plug-in in ImageJ software is shown on the right side. Movement of beads during the single-trap experiment is shown as green tracks, while that during the double-trap experiment (3.5–5.5 pN, measured by means of the displacement of the upper beads) is shown as red tracks. The difference between the starting points of single-trap and double-trap experiments ($\sim 1 \mu\text{m}$) can be attributed to the rotation of the bead due to a difference in the tensile force (Dupuis et al., 1997). The scale bar is 2 μm .

Movie 3. Phase contrast images of elongation of the bead-to-bead distance due to actin polymerization (3 μM ADP-G-actin). For color codes of tracks, see the legend to **Movie 2**. The scale bar is 2 μm .

Movie 4. Phase contrast images of elongation of the bead-to-bead distance due to actin polymerization (0.2 μM ATP-G-actin + 6 μM profilin). For color codes of tracks, see the legend to **Movie 2**. The scale bar is 2 μm .

Movie 5. Phase contrast images of elongation of the bead-to-bead distance due to actin polymerization (3 μM ADP-G-actin + 3 μM profilin). For color codes of tracks, see the legend to **Movie 2**. The scale bar is 2 μm .